

Sound modes in collisional superfluid and normal Bose gases

K. Furutani¹, A. Tononi¹, and L. Salasnich^{1,2,3}

¹ Dipartimento di Fisica e Astronomia “Galileo Galilei”, Università di Padova, via Marzolo 8, 35131 Padova, Italy.

² CNR-INO, via Nello Carrara, 1 - 50019 Sesto Fiorentino, Italy.

³ Istituto Nazionale di Fisica Nucleare (INFN), Sezione di Padova, via Marzolo 8, 35131 Padova, Italy

Abstract. We theoretically investigate sound modes in a weakly-interacting collisional Bose gas in D dimensions. Using the Landau’s two-fluid hydrodynamics and working within the Bogoliubov theory, we observe the hybridization of the first and second sound modes for $D \geq 2$. To model the recent measurements of the sound velocities in 2D, obtained around the Berezinskii-Kosterlitz-Thouless transition temperature and outside the very weakly-interacting regime, we derive a refined calculation of the superfluid density, finding a fair agreement with the experiment. In the 1D case, for which experimental results are currently unavailable, we find no hybridization, triggering the necessity of future experimental investigations. Our analysis provides a systematic understanding of sound propagation in a collisional weakly-interacting Bose gas in D dimensions.

1. Introduction

Superfluidity is one of the most interesting quantum phenomena, and serves as a reliable paradigm for the description of a wide class of quantum systems [1, 2]. The standard theoretical framework to study the superfluid properties of a D -dimensional Bose gas is Landau's two-fluid model [3, 4], in which the quantum fluid is described as a mixture of a normal component and a superfluid component. While the normal part of the fluid is viscous, the superfluid one flows without friction and does not carry entropy. A notable consequence in the near-to-equilibrium dynamics is the appearance of a second sound mode besides the "usual" first sound, as a result of an additional macroscopic degree of freedom: the superfluid.

In a 3D weakly-interacting Bose gas, due to the large isothermal compressibility of the system, the first and second sound modes hybridize [5, 6, 7, 8, 9], and a similar behaviour is also expected to occur in a 2D Bose gas [10]. In the 2D case the Mermin-Wagner theorem [11, 12] rules out the occurrence of long-range order at finite temperature [11, 12]; nonetheless the superfluid density can be finite at temperatures below the Berezinskii-Kosterlitz-Thouless (BKT) critical temperature, T_{BKT} [13, 14, 15]. At $T > T_{\text{BKT}}$, the proliferation of free vortices leads to a jump of the superfluid density [15], and results in the discontinuity of both first sound and second sound velocities. In the vicinity of the BKT transition temperature, an analysis based on the universal relations (UR) is known to describe this behaviour correctly [16, 17, 18, 19, 20]. Indeed, it has succeeded in predicting the sound velocities quantitatively in the temperature regime near T_{BKT} [21, 22, 23]. Compared to the 3D and 2D cases, there is few investigation of the first and second sound velocities at finite temperature in 1D. To obtain meaningful results in this case, which deserves a detailed analysis, it is important to establish in which temperature regime a hydrodynamic description is reliable.

In this paper, we systematically investigate the low-temperature behaviour of sound velocities in a D -dimensional weakly-interacting Bose gas. Utilizing the two-fluid hydrodynamics and the Bogoliubov theory, we compute the sound velocities in a collisional Bose gas in $D = 1, 2, 3$. We find that the hybridization, which has been predicted theoretically in a 3D Bose gas [5, 6, 9], can occur for $D \geq 2$. In particular, to work near T_{BKT} in 2D and outside the very weakly-interacting regime, we calculate the renormalized superfluid density by developing an improved approach based on Popov theory. Our theoretical results are, in this case, in good agreement with the experimental measurements of Ref. [23]. In the 1D case, the calculation of the sound velocities do not exhibit any hybridization and our quantitative predictions await experimental confirmations.

2. Thermodynamic quantities of a D -dimensional Bose gas

We start from the Helmholtz free energy of a weakly-interacting D -dimensional Bose gas, which, including the quantum correction at zero temperature, reads (we set $\hbar = k_{\text{B}} = 1$ throughout this paper)

$$\begin{aligned} F &= F_0 + F_{\text{Q}} + F_{\text{T}} \\ &= \frac{g}{2} \frac{N^2}{L^D} + \frac{1}{2} \sum_{\mathbf{p}} E_{\mathbf{p}} + T \sum_{\mathbf{p}} \ln \left[1 - e^{-E_{\mathbf{p}}/T} \right], \end{aligned} \quad (1)$$

where F_0 is the mean-field zero-temperature free energy with g is the Bose-Bose interaction strength, N is the total number of identical bosons confined in a hypercube of side L and hypervolume L^D . F_T is the low-temperature free energy with T is the absolute temperature and

$$E_p = \sqrt{\frac{p^2}{2m} \left(\frac{p^2}{2m} + 2gn \right)}, \quad (2)$$

is the Bogoliubov spectrum where $n = N/L^D$ is the D -dimensional number density and m is the mass of the atoms. We define a gas parameter in D -dimension as $\eta \equiv mgn^{1-2/D}/(2\pi)$, which is indeed identical to $T_c/(gn\zeta(D/2)^{2/D})$ for $D \geq 3$ with T_c is the critical temperature. The quantum correction F_Q in the free energy is obviously ultraviolet divergent and requires a regularization procedure. Dimensional regularization [24] for each spatial dimension leads to

$$F_Q = \begin{cases} L^3 \frac{8}{15\pi^2} m^{3/2} (gn)^{5/2} & (D = 3), \\ -L^2 \frac{m}{8\pi} \left[\ln \left(\frac{\epsilon_\Lambda}{gn} \right) - \frac{2}{\eta} \right] (gn)^2 & (D = 2), \\ -L \frac{2}{3\pi} m^{1/2} (gn)^{3/2} & (D = 1), \end{cases} \quad (3)$$

where $\epsilon_\Lambda = 4e^{-2\gamma-1/2}/(ma_{2D}^2) \gg gn$ [25] is a cutoff energy for $D = 2$ and $\gamma = 0.577 \dots$ is the Euler-Mascheroni's constant. The 2D s -wave scattering length a_{2D} is related to the 2D coupling constant as [24, 26]

$$g = \frac{2\pi}{m} \frac{1}{\ln(2/(e^\gamma k a_{2D}))}, \quad (4)$$

within the Born approximation and substituting $k = 2\pi/L$, one can obtain

$$\frac{\epsilon_\Lambda}{gn} = \frac{2\pi}{N} \frac{e^{-2\gamma-1/2+2/\eta}}{\eta}. \quad (5)$$

The pressure P is obtained as

$$P = - \left(\frac{\partial F}{\partial L^D} \right)_{N,T}. \quad (6)$$

Other thermodynamic quantities can be obtained as well from the Helmholtz free energy in Eq. (1). The entropy per mass unit and the specific heat at constant volume are given by

$$s = \frac{1}{m} \left(\frac{\partial F}{\partial T} \frac{F}{N} \right)_\rho, \quad c_V = T \left(\frac{\partial s}{\partial T} \right)_\rho. \quad (7)$$

3. Landau's two-fluid model

In Landau's two-fluid model, which allows for the calculation of the sound velocities, the collisional Bose gas is described as a mixture of a viscous normal fluid and a non-viscous superfluid. Thus, the total mass density $\rho = mn = \rho_n + \rho_s$ is composed of the

normal mass density ρ_n and the superfluid mass density ρ_s . The normal mass density is given by [3, 4]

$$\rho_n = -\frac{1}{D} \int \frac{d^D \mathbf{p}}{(2\pi)^D} p^2 \frac{dn_B(E_p)}{dE_p}, \quad (8)$$

which, for a noninteracting gas with $g = 0$, reduces to the total mass density $\rho_n = \rho$ and the superfluid fraction vanishes.

The first sound velocity u_1 and the second sound velocity u_2 ($\leq u_1$) are the solutions of the following biquadratic equation [3]

$$u^4 - (v_A^2 + v_L^2) u^2 + v_T^2 v_L^2 = 0. \quad (9)$$

In Eq. (9), we used the isothermal, adiabatic, and Landau velocity given by [3, 27]

$$v_T = \sqrt{\left(\frac{\partial P}{\partial \rho}\right)_T}, \quad v_A = \sqrt{\left(\frac{\partial P}{\partial \rho}\right)_s}, \quad v_L = \sqrt{\frac{\rho_s T s^2}{\rho_n c_V}}, \quad (10)$$

respectively.

Denoting \bar{P} as the pressure contribution which includes the mean-field plus the thermal one, and P_Q as the quantum correction, one can obtain

$$v_T = \sqrt{\left(\frac{\partial (\bar{P} + P_Q)}{\partial \rho}\right)_T} = \sqrt{\bar{v}_T^2 + v_Q^2}, \quad (11)$$

where \bar{v}_T is the isothermal velocity within the mean-field theory and

$$v_Q^2 \equiv \left(\frac{\partial P_Q}{\partial \rho}\right)_T, \quad (12)$$

is the beyond-mean-field correction to the isothermal velocity. Since F_Q is the zero-temperature free energy, it does not affect the Landau velocity v_L and the quantum correction to the adiabatic velocity is identical to that to the isothermal one as

$$v_A = \sqrt{\bar{v}_A^2 + v_Q^2}, \quad (13)$$

where \bar{v}_A is the adiabatic velocity within the mean-field theory. The explicit expressions of the quantum correction v_Q^2 are given by

$$v_Q^2 = \begin{cases} \frac{2(2\pi\eta)^{3/2}}{\pi^2} v_B^2 & (D = 3), \\ -\frac{\eta}{2} \left[\ln\left(\frac{\epsilon\Lambda}{gn}\right) - \frac{2}{\eta} - \frac{1}{2} \right] v_B^2 & (D = 2), \\ -\sqrt{\frac{\eta}{2\pi}} v_B^2 & (D = 1). \end{cases} \quad (14)$$

Fig. 1 represents the quantum correction v_Q^2 to the gas parameter η in each dimension. One can see that v_Q^2 vanishes as $\eta \rightarrow 0$ in any dimension.

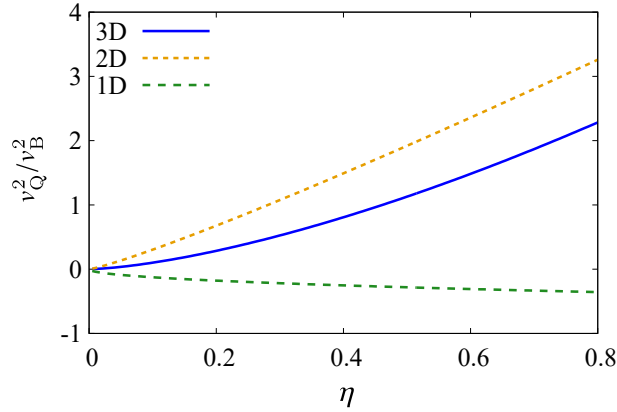


Figure 1. The beyond-mean-field correction to the isothermal and adiabatic velocity v_Q^2 for $D = 1, 2, 3$. For $D = 2$, the number of particles is set to $N = 10^4$.

3.1. Three-dimensional Bose gas

Let us discuss the propagation of the first sound and second sound in $D = 3$. The velocities of these modes are shown in Fig. 2, where the temperature is rescaled as $t = T/(gn)$ and where the Bogoliubov velocity reads $v_B = \sqrt{gn/m}$. Note that, in the main figure, we set the gas parameter to $\eta \equiv mgn^{1/3}/(2\pi) = 0.1$. At $T = 0$, as discussed in Appendix A, we reproduce the well-known result:

$$u_1 = \bar{v}_T = \bar{v}_A = v_B, \quad u_2 = v_L = \frac{v_B}{\sqrt{3}}, \quad (15)$$

which is given by mean-field theory. Around $t = 0.6$, it exhibits a hybridization of the two sound modes with a small gap. This has been pointed out by Refs. [5, 6, 7, 8, 9] for a weakly-interacting 3D Bose gas. At higher temperature than the critical temperature at which the Landau velocity vanishes, one can check that the first sound velocity coincides with the adiabatic one $u_1 = v_A$. The inset shows the first sound and second sound velocity for $\eta = 0.1$ and $\eta = 0.2$. It exhibits that a larger gas parameter opens the gap larger. In 3D, the hybridization occurs for any gas parameters. One can check this by a hybridization criterion, $v_T|_{T=0} > v_L|_{T=0}$, since the first sound and second sound velocity are the roots of Eq. (9). This inequality is satisfied for any gas parameter in 3D.

The dotted lines in Fig. 2 indicates the isothermal, adiabatic, and Landau velocity for $D = 3$. The normal density fraction ρ_n within the Landau's prescription does not include effects of interactions among elementary excitations and is a low-temperature approximation. In addition, the Bogoliubov theory is not applicable at high temperature regime comparable with T_c , so that the critical temperature at which ρ_s vanishes cannot exactly coincide with the superfluid phase transition temperature T_c [9].

These results are reliable in physical regimes where the hydrodynamic description of the system is valid. In particular, it is necessary that $\omega\tau \ll 1$ with τ is the collisional time and $\omega \simeq v_B k$ is the frequency of the excited phononic mode. The collisional time is given by

$$\tau \sim \frac{l_{\text{mfp}}}{v_{\text{th}}} \sim \frac{1}{n\sigma v_{\text{th}}}, \quad (16)$$

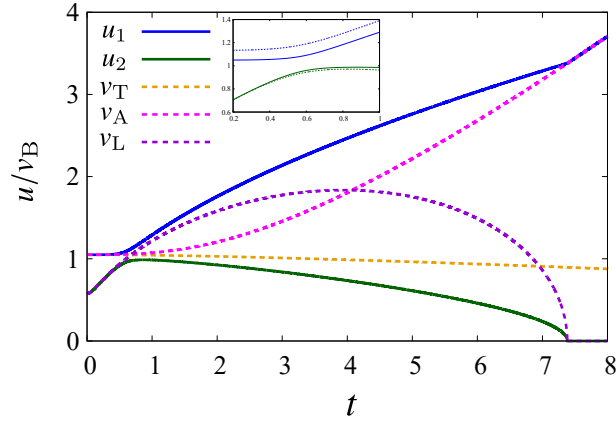


Figure 2. Results of sound velocities in a weakly-interacting Bose gas for $D = 3$ and $\eta = 0.1$. The horizontal axis is the reduced temperature $t = T/(gn)$. Inset: The hybridization of the first sound and second sound modes. The dotted lines represent the results for $\eta = 0.2$.

where $l_{\text{mfp}} \sim 1/(n\sigma)$ is the mean-free-path and $v_{\text{th}} = \sqrt{2T/m}$ is the thermal velocity. For $D = 3$, the cross-section is given by $\sigma = 4\pi a^2 = m^2 g^2 / (4\pi)$, which leads to

$$\omega\tau \sim N^{-\frac{1}{3}} \sqrt{\frac{2}{t}} \eta^{-2}. \quad (17)$$

Equation (17) indicates that our hydrodynamic description is valid at higher reduced temperature, for a large gas parameter, or for a large number of particles.

3.2. Two-dimensional Bose gas

The superfluid properties of a 2D Bose gas are crucially different from those of the 3D case due to the phenomenology of the BKT transition [13, 14, 15]. The theoretical framework developed in Sec. 2, where the topological excitations of the bosonic fluid are not taken into account, cannot describe the BKT transition. These excitations are responsible for the universal jump of the superfluid density at BKT transition temperature, T_{BKT} . To include it in our theory, we employ the KT-Nelson's formula [15]

$$\frac{\pi}{2m^2} \rho_s = T_{\text{BKT}}, \quad (18)$$

which determines the BKT transition temperature T_{BKT} . A good approximation in an infinite-size weakly-interacting system is to cut the superfluid density fraction for $T \geq T_{\text{BKT}}$.

We show the sound velocities in a 2D Bose gas in Fig. 3. Due to the jump of the superfluid density at $t = t_{\text{BKT}}$, the first sound and second sound velocity exhibit discontinuities. One can see that the hybridization of u_1 and u_2 occurs around $t_{\text{hyb}} \simeq 0.4$ for $\eta = 0.1$. Fig. 4 displays the dependence of hybridization temperature on the gas parameter η . The hybridization temperature t_{hyb} is determined by the temperature at which the difference between the first and second sound velocity starts to increase. It reveals that the hybridization temperature is different between the 3D and 2D cases. For $\eta \gtrsim 0.6$ in 2D, the hybridization temperature coincides with the

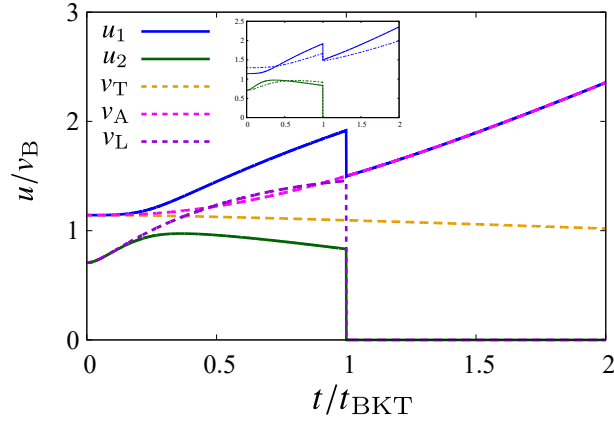


Figure 3. Results of sound velocities for $D = 2$ and $\eta = 0.1$. The number of particle is set to be $N = 10^4$. The horizontal axis is the reduced temperature scaled by the BKT transition temperature $t_{\text{BKT}} = T_{\text{BKT}}/(gn)$, which is determined by the KT-Nelson's formula in Eq. (18) for the superfluid density in the two-fluid model while ρ_n is computed by Eq. (8). Inset: The first sound and second sound velocity. The solid lines represent the results for $\eta = 0.1$ and the dotted ones represent that for $\eta = 0.2$

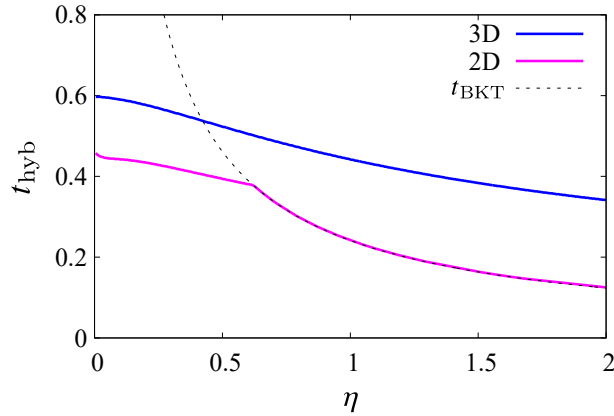


Figure 4. The hybridization temperature for $D = 3$ and $D = 2$. In the latter case, the particle number is set to $N = 10^4$. In 2D, moreover, the hybridization temperature coincides with the BKT transition temperature for $\eta \gtrsim 0.4$.

BKT transition temperature, while our analysis would not be applicable at such high temperature region comparable with t_{BKT} .

Our theoretical approach is reliable to describe the propagation of sound in weakly-interacting Bose gases, for which $mg \ll 1$, and at low temperature. The recent experiments with 2D bosonic superfluids [23], however, consider the relatively high value of $mg = 0.64$ and work near T_{BKT} , a regime which is not well reproduced by our theory. In particular, the sound velocities are strongly dependent on the superfluid density and the one derived from the Landau formula of Eq. (9) is, strictly speaking, a low-temperature approximation.

In order to describe the strongly-interacting regime of the experiments we

evaluate the renormalized superfluid density, $\rho_s^{(R)}$, by solving the Nelson-Kosterlitz renormalization group equations [15]. These differential equations describe the renormalization of the superfluid density due to presence of vortex-antivortex excitations, which are not taken into account by the Landau formula of Eq. (8). They read [15]

$$\begin{aligned}\partial_l K^{-1}(l) &= 4\pi^3 y^2(l) \\ \partial_l y(l) &= [2 - \pi K(l)] y(l)\end{aligned}\quad (19)$$

where $K(l) = \rho_s(l)/(mT)$, with $\rho_s(l)$ the superfluid density at the adimensional scale l , and $y(l) = \exp\{-\mu_c(l)/T\}$ is the fugacity, where $\mu_c(l)$ is the vortex chemical potential at scale l .

To describe consistently the finite-size experiments, we solve numerically these equations up to a finite scale, $l_{\max} = \ln(A^{1/2}/\xi)$, where A is the area of the system and $\xi = (g\rho)^{-1/2}$ is the healing length, corresponding approximately to the vortex core size. In the solution of Eqs. (19) the choice of the initial conditions is quite delicate: we choose the chemical potential of the bare vortices as $\mu_c(0) = \pi^2 \rho_s(0)/(2m^2)$ [28], and for the initial value of $K(0)$ we use $K(0) = \rho_s(0)/(mT)$, with $\rho_s(0) = \rho - \rho_n(0)$. It is important to point out that the bare Landau density which we introduce here, $\rho_n(0)$, is formally the same of Eq. (8), but is calculated with the Popov spectrum:

$$E_{p,\text{Pop}} = \sqrt{\frac{p^2}{2m} \left(\frac{p^2}{2m} + 2\mu \right)}, \quad (20)$$

where μ is the chemical potential of the system. We derive this chemical potential as a function of N and of T by inverting numerically the grandcanonical equation of state, which reads (see Ref. [25])

$$N = \frac{m\mu L^D}{4\pi} \ln \left(\frac{4}{m\mu a_{2D} e^{2\gamma+1}} \right) + \sum_{\vec{p}} \frac{p^2}{2m} \frac{n_B(E_{p,\text{Pop}})}{E_{p,\text{Pop}}}. \quad (21)$$

In particular, we evaluate a_{2D} as [26]

$$a_{2D} = 2.092 a_z \ln \left(-\sqrt{\frac{\pi}{2}} \frac{a_z}{a_{3D}} \right), \quad (22)$$

where a_z is the characteristic length of the transverse harmonic confinement and a_{3D} is the three-dimensional s -wave scattering length, which is directly controlled in the experiment [23]. The procedure described above allows us to have reliable results for $\rho_s^{(R)} \equiv \rho_s(l_{\max})$, even for relatively strong interactions and near T_{BKT} . Given the renormalized density $\rho_s^{(R)}$ for every temperature T , we use it as an input to calculate the sound velocities.

Our results are outlined in Fig. 5, which shows u_1 and u_2 in the left panel and the superfluid density $\mathcal{D}_s = n_s \lambda_T^2$ in the right panel in comparison with the experimental data [23]. As in the experiment, here we use $mg = 0.64$, the number density of $n = 3 \mu\text{m}^{-2}$ and the system area of $A = 33 \times 22 \mu\text{m}^2$ [23]. Fig. 5(a) indicates that the results using the renormalized superfluid density fraction with the exact chemical potential, represented by the blue and dark-green solid lines, agree well with the experimental values. One can see that our first sound velocity also describes the behaviour of each sound velocity at low temperature better than the

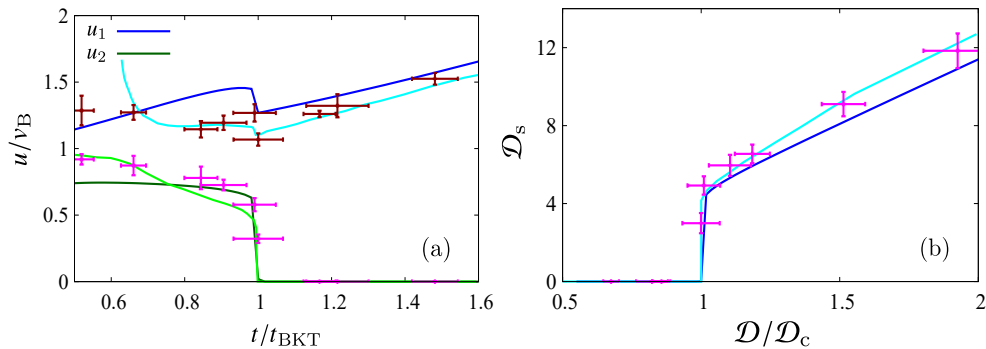


Figure 5. First sound and second sound velocities (panel (a)) and rescaled superfluid density $\mathcal{D}_s = n_s \lambda_T^2$ in 2D (panel (b)) for $mg = 0.64$, plotted in comparison with the experimental data of Ref. [23] where $D/D_c = t_{\text{BKT}}/t$. The particle number is set to be $N = 2178$ [23]. The blue and dark-green solid lines represent our results using the renormalized superfluid density [15] with the exact chemical potential. The cyan and green solid lines represent the results of UR analysis [16, 17, 18, 19, 20, 21, 22, 23].

UR analysis [16, 17, 18, 19, 20, 21, 22], which well predicts thermodynamic quantities in the vicinity of T_{BKT} . The slight deviation of our second sound velocity from the experimental one at low temperature is just ascribed to the inconsistency between the thermodynamic quantities calculated under the low-temperature approximation $\mu = gn$ and the renormalized superfluid density $\rho_s^{(R)}$ with the exact μ that appear in Eq. (10). Fig. 5(b) displays that the renormalized \mathcal{D}_s with the exact chemical potential agrees well with the experimental values.

As in the 3D case, we now discuss the validity of the hydrodynamic description. The cross-section for $D = 2$ is given by $\sigma \sim (2\pi\eta)^2 / (mv_{\text{th}})$ and the adimensional collisional time is independent of the temperature as

$$\omega\tau \sim \frac{1}{\sqrt{2\pi N}} \eta^{-\frac{3}{2}}. \quad (23)$$

Equation (23) indicates that the hydrodynamic description for $D = 2$ is valid for a large gas parameter or a large number of particles. In the experimental observation reported in Ref. [23], the gas parameter and the number of particles are $\eta \simeq 0.10$ and $N \simeq 2178$, and one obtains $\omega\tau \simeq 0.26$, in which our hydrodynamic description is reliable.

3.3. One-dimensional Bose gas

On the basis of the Mermin-Wagner theorem [11], the critical temperature T_{BEC} below which there is Bose-Einstein condensation, or equivalently below which there is off-diagonal long-range order (ODLRO), is positive in 3D, it is zero in 2D, and it is absent in 1D. Instead, the critical temperature T_c below which there is superfluidity, or equivalently below which there is algebraic long-range order (ALRO), is equal to T_{BEC} in 3D, it is equal to T_{BKT} in 2D, and it is zero in 1D. Thus, in the thermodynamic limit and with $T > 0$, for a 1D weakly-interacting Bose gas there is neither ODLRO nor ALRO. However, a finite 1D system of spatial size L is effectively superfluid [29] if $T \ll E_\phi / \ln(L/\xi)$, or equivalently $t \ll t_\phi \equiv 1 / [\sqrt{\pi}\eta \ln(2N\sqrt{\pi}\eta)]$, where

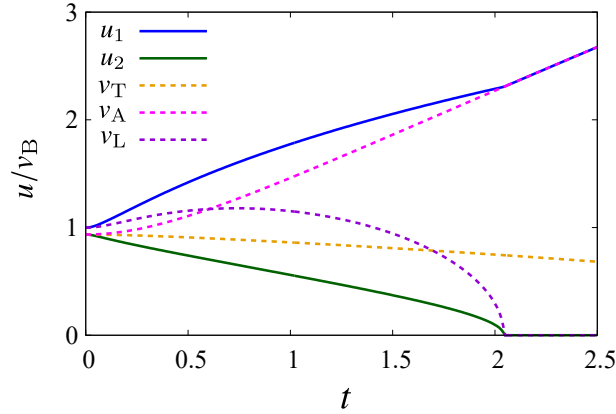


Figure 6. Results of sound velocities for $D = 1$ and $\eta = 0.1$. The horizontal axis is the reduced temperature $t = T/(gn)$.

$E_\phi \simeq n/(m\xi)$ is the energy to create a phase slip (black soliton) and ξ is the corresponding healing length. Note that, for $\eta \ll 1$, the adimensional temperature t_ϕ can be quite large.

In Fig. 6, we show also the results of u_1 and u_2 in an 1D Bose gas. The figure exhibits no hybridization of u_1 and u_2 because $u_1 = u_2 = v_B$ at zero temperature within the mean-field and the gap at zero temperature between u_1 and u_2 opens by including the quantum correction. One can also check the absence of hybridization by $v_T|_{T=0} < v_L|_{T=0}$ for any gas parameter in 1D.

4. Conclusion

We discussed sound modes in a collisional Bose gas in D -dimension by means of the Landau's two-fluid hydrodynamics and the Bogoliubov theory. We found the occurrence of the hybridizations between the first and second sound for $D \geq 2$. In a 3D Bose gas, it occurs for any gas parameter. Similar hybridization of the first and second sound occurs also in 2D. In comparison with the experimental observation by Ref. [23], we found that our refined results with the renormalized superfluid density and the exact chemical potential are in fair agreement with the measured values associated with the relatively strong interactions of the realized experimental setup. Furthermore, differently from the universal relations analysis, it predicts the first sound velocity quantitatively better in the low-temperature regime. This indicates that our theoretical approach would be reliable for the predictions of experimental measurements in the whole temperature region. We computed the velocities also in 1D and found no hybridization. Since there are no available experimental data yet in this configuration, our 1D analysis could provide a benchmark for future investigations.

Acknowledgments

We thank J. Schmitt, M. Ota, and V. Singh for providing the experimental and theoretical data. KF acknowledges Fondazione Cassa di Risparmio di Padova e Rovigo for a PhD scholarship.

Appendix A. Sound velocity in the phononic regime

At very low temperature, according to Ref. [3], and under the condition $g \neq 0$, all the thermodynamic functions are fixed by the thermal excitations of the phonons and consequently the Bogoliubov spectrum can be approximated as

$$E_p = v_B p. \quad (\text{A.1})$$

In this phononic regime, within the framework of mean-field theory, one can perform the momentum integral in Eq. (1) analytically as

$$\frac{F}{N} = \frac{g\rho}{2m} - \frac{\Omega_D \Gamma(D) \zeta(D+1)}{(2\pi)^D} \frac{m^{D+1}}{g^{D/2} \rho^{D/2+1}} T^{D+1}, \quad (\text{A.2})$$

$$P = \frac{g\rho^2}{2m^2} + \left(\frac{D}{2} + 1\right) \frac{\Omega_D \Gamma(D) \zeta(D+1)}{(2\pi)^D} \frac{m^D}{g^{D/2} \rho^{D/2}} T^{D+1}, \quad (\text{A.3})$$

where $\Omega_D = D\pi^{D/2}/\Gamma(D/2+1)$ is the volume of the D -dimensional unit sphere with $\Gamma(x)$ the Euler gamma function and $\zeta(x)$ the Riemann zeta function. The entropy per mass unit, specific heat, and normal density fraction are obtained as

$$s = (D+1) \frac{\Omega_D \Gamma(D) \zeta(D+1)}{(2\pi)^D} \frac{m^D}{g^{D/2} \rho^{D/2+1}} T^D, \quad (\text{A.4})$$

$$c_v = (D+1) D \frac{\Omega_D \Gamma(D) \zeta(D+1)}{(2\pi)^D} \frac{m^D}{g^{D/2} \rho^{D/2+1}} T^D, \quad (\text{A.5})$$

$$\rho_n = (D+1) \frac{\Omega_D \Gamma(D) \zeta(D+1)}{(2\pi)^D} \frac{m^{D+2}}{g^{D/2+1} \rho^{D/2+1}} T^{D+1}. \quad (\text{A.6})$$

Using Eqs. (9), (10), at zero-temperature within the mean-field theory, one obtains

$$u_1 = \bar{v}_T = \bar{v}_A = v_B, \quad u_2 = v_L = \frac{1}{\sqrt{D}} v_B. \quad (\text{A.7})$$

- [1] Pethick C J and Smith H 2002 *Bose-Einstein Condensation in Dilute Gases* (Cambridge: Cambridge University Press)
- [2] Pitaevskii L and Stringari S 2016 *Bose-Einstein Condensation and Superfluidity* (Oxford: Oxford University Press)
- [3] Landau L D 1941 *J. Phys. (USSR)* **5** 71
- [4] Landau L D and Lifshitz E M 1987 *Fluid Mechanics* (Oxford: Pergamon)
- [5] Lee T D and Yang C N 1959 *Phys. Rev.* **113** 1406
- [6] Griffin A and Zaremba E 1997 *Phys. Rev. A* **56** 4839
- [7] Taylor E, Hu H, Liu X -J, Pitaevskii L P, Griffin A, and Stringari S 2009 *Phys. Rev. A* **80** 053601
- [8] Hu H, Taylor E, Liu X -J, Stringari S, and Griffin A 2010 *New. J. Phys.* **12** 043040
- [9] Verney L, Pitaevskii L, and Stringari S 2015 *EPL* **111** 40005
- [10] Singh V P and Mathey L arXiv:2010.00013
- [11] Mermin N D and Wagner H 1966 *Phys. Rev. Lett.* **17** 1133
- [12] Hohenberg P C 1967 *Phys. Rev.* **158** 383
- [13] Berezinskii V L 1972 *Sov. Phys. JETP* **34** 610
- [14] Kosterlitz J M and Thouless D J 1972 *J. Phys. C* **5** L124 ; 1973 *J. Phys. C* **6** 1181
- [15] Nelson D R and Kosterlitz J M 1977 *Phys. Rev. Lett.* **39** 1201
- [16] Prokof'ev N, Ruebenacker O, and Svistunov B 2001 *Phys. Rev. Lett.* **87** 270402
- [17] Prokof'ev N and Svistunov B 2002 *Phys. Rev. A* **66** 043608
- [18] Yefsah T, Desbuquois R, Chomaz L, Günter K J, and Dalibard J 2011 *Phys. Rev. Lett.* **107** 130401

- [19] Hung C -L, Zhang X, Gemelke N, and Chin C 2011 *Nature* **470** 236
- [20] Rançon A and Dupuis N 2012 *Phys. Rev. A* **85** 063607
- [21] Ozawa T and Stringari S 2014 *Phys. Rev. Lett.* **112** 025302
- [22] Ota M and Stringari S 2018 *Phys. Rev. A* **97** 033604
- [23] Christodoulou P, Galka M, Dogla N, Lopes R, Schmitt J, and Hadzibabic Z arXiv:2008.06044
- [24] Salasnich L and Toigo F 2016 *Phys. Rep.* **640** 1
- [25] Mora C and Castin Y 2009 *Phys. Rev. Lett.* **102** 180404
- [26] Dalibard J 2016 *Fluides quantiques de basse dimension et transition de Kosterlitz-Thouless* (Collège de France Lecture Notes)
- [27] Khalatnikov I M 1965 *An Introduction to the Theory of Superfluidity* (New York: Benjamin)
- [28] Bighin G and Salasnich L 2017 *Sci. Rep.* **7** 45702
- [29] Svistunov B, Babaev E, and Prokof'ev N 2015 *Superfluid States of Matter* (Boca Raton: CRC Press)